LOW-DEFLECTION LOSS AND HYSTERESIS MEASUREMENTS ON A SPACECRAFT TEST JOINT

Eric M. Austin*
CSA Engineering, Inc.
Palo Alto, California

Timothy L. Flora
Lockheed Missiles and Space Company, Inc.
Sunnyvale, California

James C. Goodding
CSA Engineering, Inc.
Palo Alto, California

ABSTRACT

Passive damping has been demonstrated to be an effective and efficient means for limiting the effects of on-board excitations on the dynamics of space vehicles. High-precision applications require these treatments to both be effective at very low excitation levels and not affect the dimensional stability of the structure under quasi-static and thermal-mechanical loads. This work documents a study of two important issues facing structures damped with viscoelastic materials: hysteresis and loss at low deflection levels.

The test article is an I-beam-like structure designed to simulate an experimental method of fabricating graphite-epoxy/honeycomb structures without using any mechanical fasteners. After identifying the most critical vibrational modes from a separate system-level analysis, a damping treatment was designed for the test joint using standard finite element techniques. A modal test using very low random excitation levels was performed on the resulting damped structure. Statistical methods were used to determine that the maximum displacement level of the free-free structure was of the order of nano-meters. Subsequently, hysteresis tests were performed on the same damped beam. Laser interferometry was used to measure displacements of the joint after undergoing cyclic static loads of varying magnitudes. Percent hysteresis was measured while the joint was loaded in three-point bending. Hysteresis behavior during displacements as small as 150 nano-meters was recorded.

*Senior Engineer, 560 San Antonio Road, Suite 101, Palo Alto, CA 94306 (415) 494-7351

1. Introduction and Objectives

Passive damping has been demonstrated to be a vital technology for limiting the effects of on-board excitations on the dynamics of space vehicles. High-precision applications require these treatments to both be effective at very low excitation levels and not affect the dimensional stability of the structure under quasi-static and thermal-mechanical loads. Of equal concern are the damping characteristics of the structure when undergoing very low strain levels. This information is particularly important when performing analysis of the structure to predict response to launch and in-service loads. Since this fabrication technique is new, typical levels of inherent damping are not known. It is also anticipated that passive damping will be incorporated into any design using this construction technique, so it is necessary to test for damping performance at very low levels of response.

For many spacecraft designs it is desirable to predict the magnitude the structure may deform or shift after being launched and placed in service. This deformation can be caused by gravity release or changes to the thermal and moisture environment. However, one of the largest and least understood contributors is hysteresis. Structural hysteresis is the failure of the structure to return to its original position after an external load has been applied and removed. This effect is typically caused by friction effects, slippage of fasteners within their holes, and small viscoelastic properties of most materials. Hysteresis is not to be confused with inelastic behavior of a structure resulting from loads exceeding the yield strength or proportional limit. It is also separated from the predictable effects of both long-term creep, where materials deform slowly due to sustained stresses, and microcreep, which occurs when repeated short-term loading exceeds the material's microyield strength.[1] In essence, hysteresis is treated herein as an accumulation of distortion sources that cannot be accounted for by classical analysis techniques.

Of particular concern is the behavior of dimensionally critical spacecraft structures. Hysteresis predictions of precision composite structures after being launched or after small on-orbit maneuvering loads are applied must be based on limited and mostly irrelevant static test data. The hysteresis of structures constructed using graphite/epoxy parts bonded together with honeycomb core is not well understood. When viscoelastic passive damping materials are applied, the hysteresis of the structure may increase, especially during low-amplitude vibration. The hysteresis test is designed to give insight into these problems and aid in analysis efforts to bound or quantify structural hysteresis behavior. In summary, the objectives of the hysteresis tests are as follows:

1. Measure the amount of hysteresis present in a generic spacecraft joint with a constrained layer passive damping treatment applied.

2. Determine the linearity of hysteresis at low displacement levels.

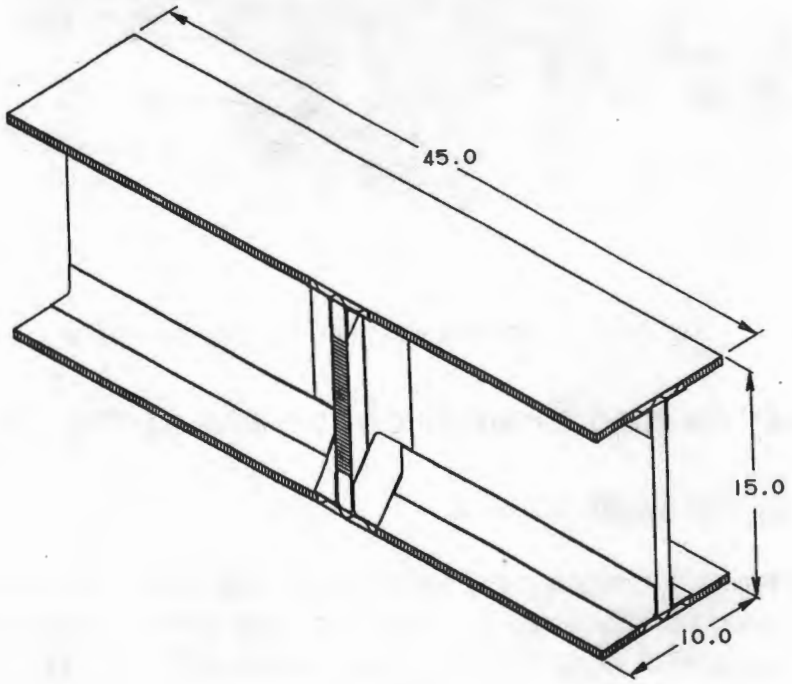

Figure 1. Sketch of the test article

The test article, shown in Figure 1, is designed to simulate an experimental method of fabricating graphite-epoxy/honeycomb structures without the use of any mechanical fasteners. The article is essentially the intersection, a joint, between two composite I-beams at an angle of 60°. The attachments are strengthened with overlapping graphite-epoxy (GR/EP) plates attached solely with high-strength epoxies. The primary mode of interest is the first bending mode of the "I-beam" in its strong direction, since that deflection best simulates operational deflections using this construction.

A secondary objective of this effort was to design and apply an add-on damping treatment that would increase the damping of the test article significantly in the mode of interest. A finite element model was developed to aid in this design. The finite element model was constructed with enough details that it could be used later for failure analysis of some of the internal parts. This configuration was also tested at very low levels of excitation.

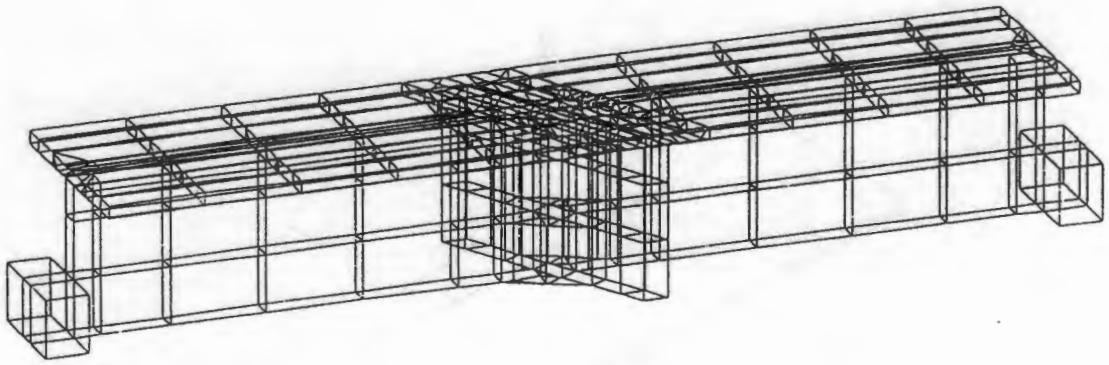

Figure 2. Finite element model of the test joint

2. Analysis and Design of the Damping Treatment

2.1 Finite Element Model

The primary reason for creating the finite element model was to evaluate candidate damping treatments for the test joint. The model was based on drawings supplied by LMSC and was created using I-DEAS pre-processing software. The finished model was translated from I-DEAS to MSC/NASTRAN format for the actual analyses. Figure 2 shows the resulting finite element model. Due to symmetry, only half of the structure was modeled.

2.2 Predicted Baseline Modes

The modes of interest are the first overall mode of the Test Joint and the first bending about its strong axis, shown in Figure 3. The "banana" mode is most representative of a typical troublesome mode in similar structures. Since only half of the test joint was modeled, two runs, one with symmetric and one with asymmetric boundary conditions, are needed to predict all of the structure's modes. Both of the modes of interest are asymmetric with respect to the symmetry plane, so most of the runs were done using only these boundary conditions. Since no other boundary conditions were applied, this predicted free-free modes of the test joint.

The initial run of the test joint model predicted the "banana" mode to be the eleventh elastic mode, at a frequency of slightly more than 1,200 Hz. The high frequency itself is not a problem for testing; however, the bending mode was coupled with local modes of nearly every panel section in the structure. This would have complicated the test greatly, requiring many measurement points in order to identify the proper mode with confidence. Another concern was that the high level of local panel participation might distort the inherent level of damping sought for the pure "banana" mode.

The solution agreed upon by LMSC and CSA engineers was to add some dead weight to the ends and center of the test joint. It was felt that this would bring the

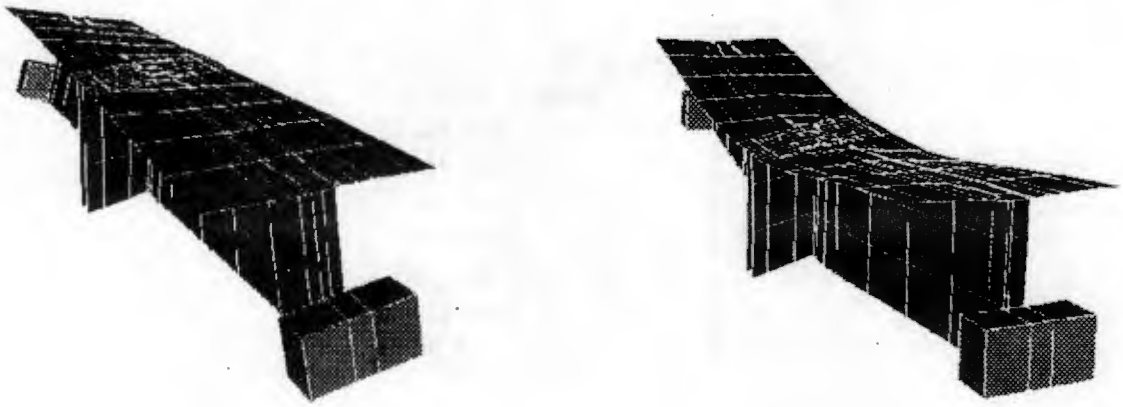

170 Hz 500 Hz

Figure 3. Primary vibration modes of interest

first bending mode down in frequency while not affecting the local panel modes. The finite element model bore this hypothesis out. The solution was to add 10 pounds to each of the ends and the center, a total of 30 pounds of added weight for the **half** model. The added weight brought the mode of interest down to about 585 Hz, and there was no local panel participation at all.

The frequencies predicted for the baseline undamped structure including the dead weight are given in Table 1.

2.3 Analysis of Damping Treatments

An ideal outcome of the this analysis would be a damping treatment that added significant damping without any additional weight. A more realistic goal is to maximize the damping added to the mode of interest while minimizing the added weight. Though there are many possible weight-efficient damping strategies, most requiring that the VEM be an integral part of the structure. A simple constrained-layer approach was chosen for this work because of hysteresis and creep concerns.

The baseline finite element model including the added weights was altered to add the effects of constrained-layer damping treatments on both the top of the flange and the sides of the webs. The damping was predicted using the Modal Strain Energy Method. Initial runs showed that the modal strain energy (MSE) in the VEM on the sides (web) was much higher that that in the VEM on the top (flange). Thus, the treatment on the flange was removed in order to save weight, and all subsequent iterations were on the web treatment only.

Mode	BC	frequency
1	asym	169 Hz*
2	sym	204 Hz
3	sym	360 Hz
4	sym	423 Hz
5	asym	514 Hz
6	asym	585 Hz†
7	sym	640 Hz
8	asym	675 Hz

* first twisting mode
† first bending, strong direction

Table 1. Predicted elastic modes of the baseline test joint

It is often logical to make the constraining layer from the same material as the base structure, especially when considering thermal expansion. LMSC had some surplus 48-mil-thick GR/EP from the same batch used on the test joint, so this was chosen for the constraining-layer material. It was shown through analysis that increasing the thickness from 48 to 96 mils (milli-inches) did not increase the damping enough to justify the increase in weight. Thus, the final constraining layer was a 18.5-inch-long by 9.5-inch-wide, 0.048-inch-thick sheet of graphite/epoxy, supplied by LMSC.

The next step was to determine the best combination of VEM shear modulus and thickness. The properties (shear modulus and loss factor) of viscoelastic materials vary with both temperature and frequency, and both are important in choosing a good design. The loss factor is essentially the efficiency with which strain energy in the VEM is dissipated, i.e., a low loss factor will result in low damping.

The initial candidate VEM's were chosen for their availability. The properties of these candidate were then evaluated at 585 Hz and 70°F, the approximate temperature of CSA's laboratory. Shear moduli of the VEM's having good loss factors ($\approx$>0.7) were simulated on the model, and damping was predicted following the MSE method. The viscoelastic material chosen for this application was 3M's Y-9473, a 10-mil-thick double-back adhesive transfer tape. This choice resulted in the most modal strain energy in the VEM given the other factors that were held constant.

The surface area of coverage of the treatment was approximately 700 in^2 (four sheets at 9.5 x 18.5 inches each), and the VEM has a density of about 0.035 $\frac{lb}{in^3}$. Together with the constraining layer, the added weight is about 2.5 lbs.

2.4 Predicted Levels of Damping

Once the final configuration of the damping treatment was chosen, predictions of damping were made. These damping levels, presented here in terms of viscous damping ($\frac{1}{2Q}$), were calculated using the modal strain energy in the VEM as predicted by the finite element model. The only modes of interest were the first mode overall of the system and the first bending mode in the strong direction ("banana"). From Table 1, the frequencies of these modes were predicted to be 169 and 585 Hz. Since the properties of viscoelastic materials (VEM's) are sensitive to changes in temperature and frequency, two runs had to be made for each set of symmetry conditions: one each with the VEM properties evaluated at 169 and 585 Hz. The shear modulus of the chosen VEM is nearly twice as stiff at 585 Hz as it is at 169 Hz.

The damping predicted for these two modes was 2.3% and 2.4%, respectively. A full summary of the frequencies and damping values will be included in a later section. Note that these predictions are for added damping, and they neglect any damping inherently in the structure.

3. Modal Testing of the Test Joint

3.1 Test Setup

The Test Joint was suspended with steel cables and extension springs to simulate free-free boundary conditions. In order for these boundary conditions to be effective, the rigid-body modes of the structure need to be about ten times lower in frequency that the first elastic mode. Free-free boundary conditions were chosen to reduce the possible effects of fixturing dynamics on the damping measurements. Often times with simply supported or fixed-end boundary conditions, it is difficult, if not impossible, to distinguish between loss from the structure and loss from connections at the boundary conditions. This is particularly important in a precision structure such as this where few mechanical fasteners are used. An additional benefit is that comparisons with finite element models are easier since the dynamics of the supports do not have to be modeled.

The 60 pounds of lead were added by affixing lead blocks to the ends and center of the beam. The center blocks were attached with epoxy, and the end blocks were bolted to an aluminum bar with two 3/8-inch-diameter bolts. The added weights were placed as close as possible to the center line of the Test Joint to avoid affecting twisting modes.

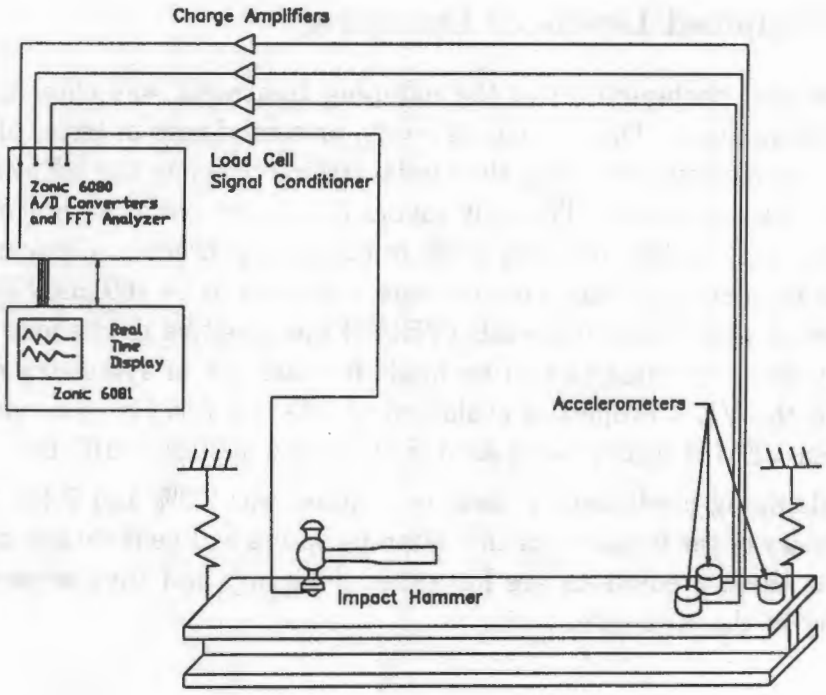

Figure 4. Schematic of test instrumentation

3.2 Instrumentation

The instrumentation for the test consisted of an impact hammer, a signal conditioner for the load cell, three piezoelectric accelerometers, accelerometer charge amplifiers, and a four-channel modal analysis system. An impact hammer was used to excite the Test Joint, since it was adequate for the measurements sought, and it doesn't require any additional fixturing or rigging.

Coupled with the charge amplifiers, the sensitivity of the accelerometers was more than adequate to ensure a good signal-to-noise ratio, even for the low-amplitude measurements. The tip on the impact hammer was chosen to input the most energy over the frequency band of interest. A schematic of the instrumentation is shown in Figure 4.

3.3 Measurements

Two points were used for most of the testing: one on the top of the Test Joint near the center line and one on the vertical web near its intersection with the flange. Two points were used since it was difficult to excite both the lowest mode (a twisting mode) of the structure and the first strong-direction bending with the same excitation, especially when impacting normal to the surfaces of the test joint. Using two

excitation points also simplified the task of data reduction, since few if any of the symmetric modes were excited by the excitation directly on top of the test joint. Recall from Table 1 that both the modes of interest are asymmetric modes.

Impact force and acceleration time records were captured and averaged with a Fast-Fourier-Transform analyzer within the test system. From these, frequency response functions (FRF's) were computed by dividing the accelerations by the excitation force. These FRF's yield insight into the test joint's structural dynamics by depicting the magnitude and phase relationships of the two signals versus frequency. Modal surveys were conducted using two impact points. Each impact point was chosen to excite one of the two modes of interest.

A standard modal analysis curve-fitting technique was used to determine the structure's resonant frequencies, the corresponding mode shapes, and the modal damping from the impact test measurements. This circle-fitting technique estimates the mode shapes by minimizing the least-square error to the FRF displayed in the complex plane. Fast-Fourier-transform zoom techniques were used to provide the very high spectral resolution required for accurate damping measurements from the data.

4. Damping at Low Displacement Amplitudes

After the modal tests had been completed, both the baseline and treated configurations were tested at low excitation levels to determine how damping was effected. The goal was to measure the damping at displacement levels of about 10 nano-meters peak-to-peak. The primary mode of interest for low-amplitude damping was the strong-direction bending ("banana") mode. It was necessary to make certain approximations and assumptions in order to determine the amplitude of the response contributed by this mode.

The test of the baseline undamped structure was done using the same impact-hammer technique used for the modal test, only with much lower impact levels and a higher sensitivity hammer tip. The response measured at the geometric center of the joint on the top surface was used as the maximum displacement. If the structure is excited on the top surface directly over the web, the desired bending mode dominates the response. Thus, it is assumed that the acceleration time history is due solely to the response of the bending mode. This allows the peak-to-peak displacement to be defined as the peak-to-peak acceleration integrated twice, i.e., divided by the square of the frequency of the mode. In order to get the low response levels, the structure was excited near the a node of the bending mode. Even if other modes were excited by the impact, the they would only add to the measured response. Thus, these displacement levels are conservative in the worst case.

After the damping treatment was applied, the excitation for the low-amplitude measurements was changed from an impact hammer to a burst-random signal applied

	Lowest Mode		Bending Mode	
	Freq (Hz)	ζ	Freq (Hz)	ζ
predicted	169	n/a	585	n/a
measured	160	0.26%	508	0.28%

Table 2. Comparison of predicted and measured frequencies and damping for the untreated baseline Test Joint

through a small shaker. The change resulted in much better quality data.

A burst-random signal was used to excite the structure with random levels of energy at all of the frequencies with a specified range. For these tests, the range was set to 160 to 640 Hz. For accuracy, several bursts are averaged to arrive at the final frequency response functions. The major drawback to this method for this application is that there no way to get an exact deterministic output from a random input. There is, however, a method for handling problems such as this. It is based on a statistical relationship between the RMS (root mean square) of a function and its peak value. This factor, sometimes called the *crest factor*, usually has a value between 3.0 and 4.0.[2,3] Additional details about the application of the crest factor for this test will be presented along with the results in the following section.

5. Test Results

After testing with various bolt configurations (different torques, different washers, grease, etc.), the original configuration was maintained for all of the testing.

5.1 Damping Measured in the Baseline Test Joint

A frequency of 160 Hz was measured for the lowest mode. This compares well with the predicted value of 169. For the "banana" mode, the measured frequency was 508 Hz, compared to 585 Hz predicted. This 15% discrepancy is of some concern, but not much since there is high confidence in the actual mode shape. Damping predictions via the modal strain energy method are dependent solely on the system eigenvectors and the structure's stiffness matrix. Of the two, the mode shape is the more important in getting accurate predictions of damping. For this reason, only minimal time was spent trying to match the frequencies of the finite element model to those measured. (A subsequent finite element model built by LMSC was tuned to match both of these modes very well.)

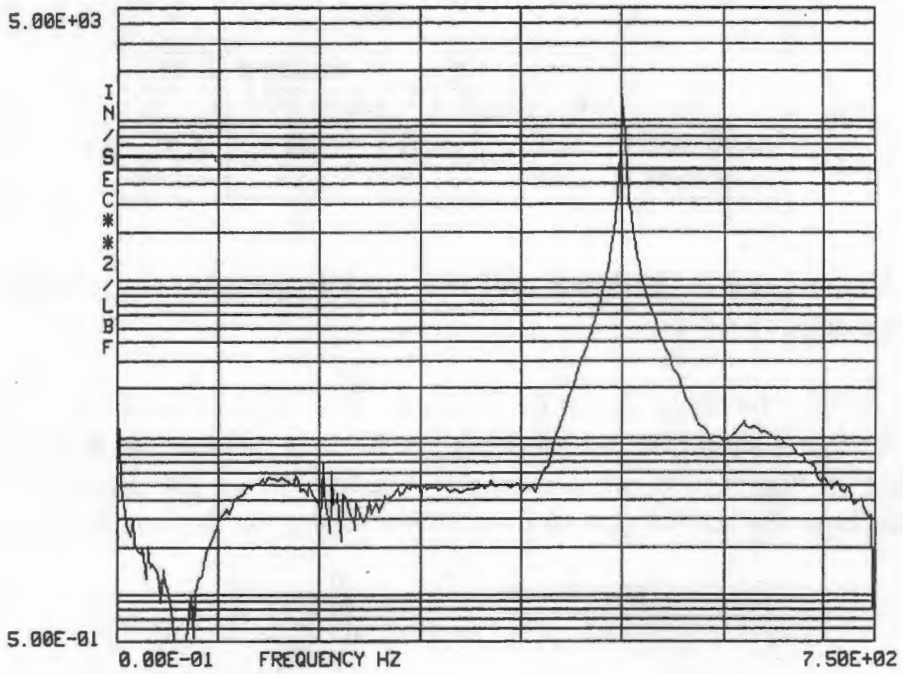

Figure 5. Frequency-response function showing strength of mode at 500 Hz

5.2 Damping Measured in the Treated Test Joint

After the damping treatment was applied, the measurements were repeated, only this time at a smaller subset of the original 32 points. The 500-Hz bending mode is very dominant when impacting the joint in the vertical direction from the top side, so it was not necessary to re-find the mode. This dominance is seen by the relative isolation (as in distance from other modes) of the mode, as shown in Figure 5. A comparison of the measured and predicted frequencies and damping values is given in Table 3. This close agreement between test and analysis damping levels is good considering that the viscoelastic material properties were not verified by test. The model correlates better with the lowest modes than with the target bending mode. Therefore, it is reasonable to expect the damping prediction for this mode to be better.

5.3 Damping Measured at Low Amplitude Levels

5.3.1 Untreated Baseline Structure

In order to produce the low-level responses desired, the Test Joint had to be excited with a light impact hammer to produce very low forces. The untreated Test Joint was excited with two low-level excitations: one producing about 25 nm zero-to-peak displacement and the other about 5 nm. The acceleration time history produced by

	Lowest Mode		Bending Mode	
	Freq (Hz)	ζ	Freq (Hz)	ζ
predicted	170	2.3%	612	2.4%
measured	169	2.5%	530	1.95%

Table 3. Comparison of predicted and measured frequencies and damping for the treated Test Joint

one of the impact forces is shown in Figure 6. The displacement was calculated as follows: The figure shows the zero-to-peak acceleration to be about 2 $\frac{in}{sec^2}$. Considering the FRF in Figure 5, it can reasonably be asserted that this signal is dominated by the 530-Hz mode, so the zero-to-peak displacement can be calculated to be

$$\begin{aligned} \text{displacement} &= \frac{\text{acceleration}}{(2\pi f)^2} = \frac{2.0\frac{in}{sec^2}}{(2\pi 530)^2 \frac{1}{sec^2}} = \\ &= 1.804 \times 10^{-7} \text{ inches} \times \frac{0.0254 \times 10^9 \text{ nano-meters}}{1 \text{ inch}} \\ &= 4.59 \text{ nano-meters} \end{aligned}$$

The damping measured for the 5-nm and 25-nm displacements was 0.28% and 0.33%, respectively. These compare very well with the 0.28% from Table 2.

5.3.2 Structure With Damping Treatment

This test used a shaker producing a burst-random signal. The quality and repeatability of the results far exceeded that of the impact hammer. As discussed briefly in a earlier section, a statistical relationship had to be employed in order to infer displacements from the random loading used on the treated structure. Two quantities are needed to determine this *crest factor*: the ratio of the RMS of a power spectral density function (PSD) at a point and the maximum response at that point. For this purpose, the acceleration at the geometric center of the top surface was used. As with the displacements, deterministic accelerations cannot be determined from a random loading. In place of finding the maximum acceleration during the random burst, a limiting value was determined. This was done by placed a limit on the voltage signal output by the accelerometer at the response point. If this limit voltage was exceeded, the ensemble was rejected. Knowing the accelerometer's relationship between acceleration and voltage output, this provides a good, if slightly conservative, measure of the maximum acceleration.

The crest factor was calculated for each excitation level by dividing the upper-limit acceleration by the RMS of the acceleration PSD between 160 and 640 Hz. This ratio was then multiplied by the RMS of the displacement PSD to obtain a statistical

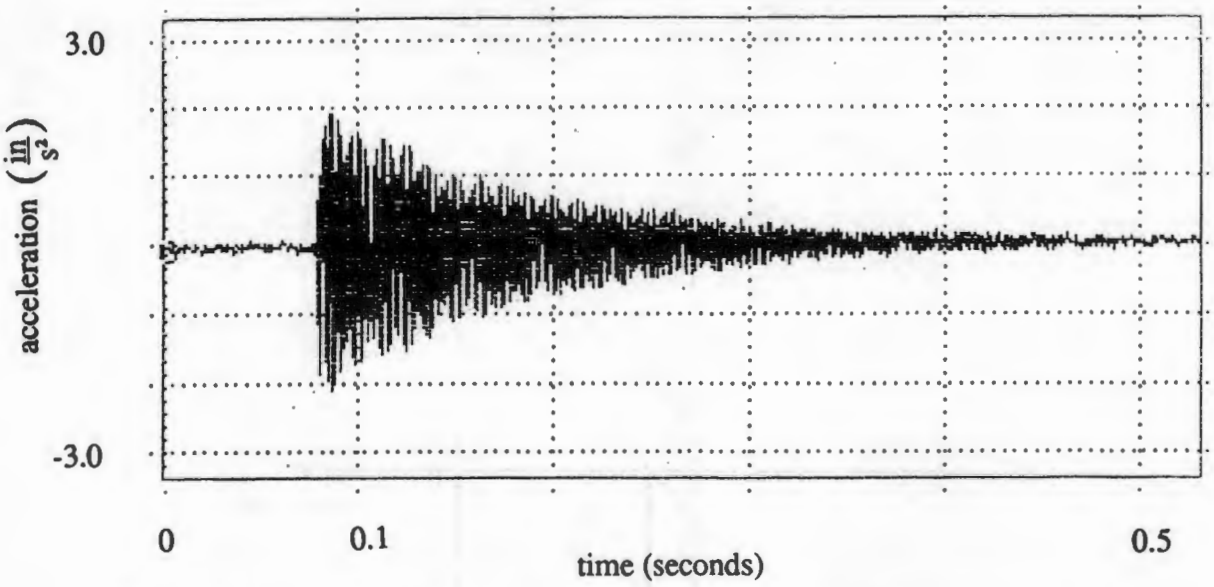

Figure 6. Acceleration time trace of low-level impact in the untreated baseline Test Joint: first strong-direction bending mode

estimate of the maximum displacement. In order to better estimate the maximum displacement of bending mode alone, the displacement RMS was computed between the half-power (3-db down) points. The results are summarized in Table 4.

In two of the measurements (marked by $*$ in Table 4), the random signal was limited to a narrow band around the desired mode. This further ensured that only the bending mode was excited. This is noted because the crest factors for these two cases are lower than the others. In the limit, as the frequency band collapses down to a single frequency, the crest factor approaches the one over the RMS of a simple sinusoid, or $\sqrt{2}$.

a_{limit} (in/s^2)	acceleration RMS (in/s^2)	Crest factor (unitless)	displacement RMS (nano-meters)	d_{limit} 0-pk (nm)	ζ (%)
0.259	0.06317	4.100	0.1042	0.427	1.77
0.386	0.1001	3.856	0.1623	0.626	2.04
0.66	0.1751	3.769	0.2937	1.11	1.95
1.93	0.7039	2.742	1.1784	3.23	1.95
5.8	2.821	2.056*	4.9863	10.25	2.04
9.65	2.538	3.802	4.148	16.8	1.95
19.3	5.043	4.808	9.270	44.57	1.95
38.6	10.99	3.51	20.163	70.82	1.95
58.0	27.75	2.090*	47.90	100.11	1.96

* band-limited signal used

Table 4. Results of test of treated joint at low excitation levels

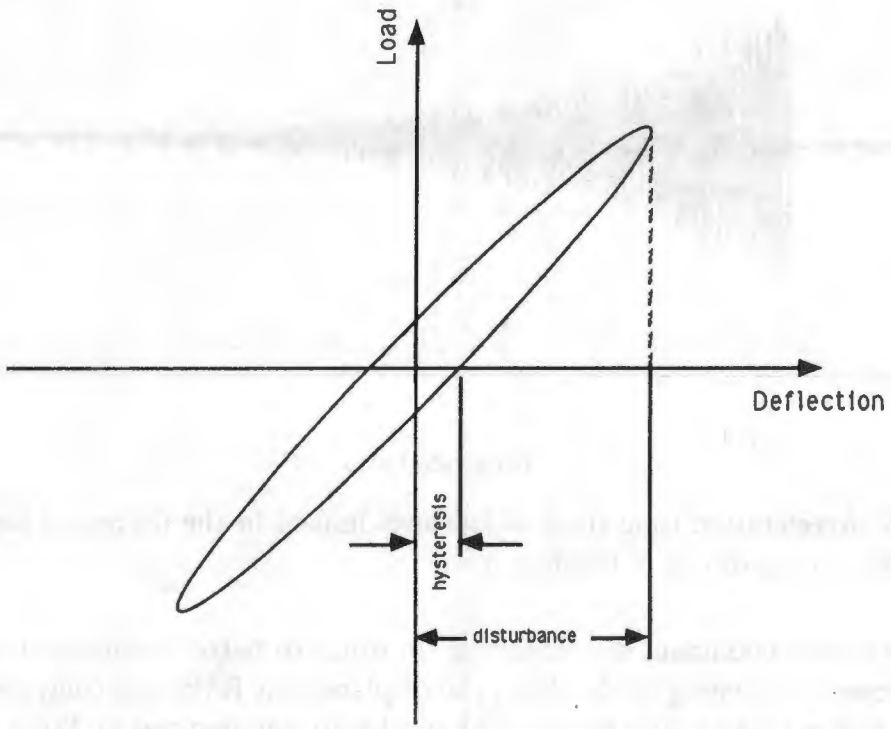

Figure 7. Percent hysteresis taken from ratio of hysteresis over disturbance

6. Hysteresis Testing

Historically on LMSC structures, hysteresis observed in static test programs typically exceeds 10% of their maximum displacements. On structures such as this where dimensional stability is of concern, hysteresis must be reduced by eliminating mechanical fasteners where possible and bonding or welding critical interfaces. Past experience with alignment platforms and other precision structures has shown hysteresis effects reduced to approximately 1% when a large static load is applied.

Quantifying hysteresis as a percent of displacement is the best method of describing the effect. It is not to suggest that hysteresis can be predicted accurately in this manner, rather the effect can be bounded by some ± percent range. This allows the effect to be accounted for within structural stability budgets.

Duration of the applied loading should not be of importance since creep effects generally take a comparatively large amount of time to accumulate and are treated separately from hysteresis. Figure 7 shows that hysteresis is independent of time. However, because graphite/epoxies respond with small viscous effects, a finite amount of time to settle and take readings was given to allow full recovery. Because of the dynamic and cyclic nature of load conditions of primary interest to spacecraft structures, the viscous behavior is not as critical as it first may seem. At any rate, because of the sensitive nature of the test equipment in use, time dependant effects

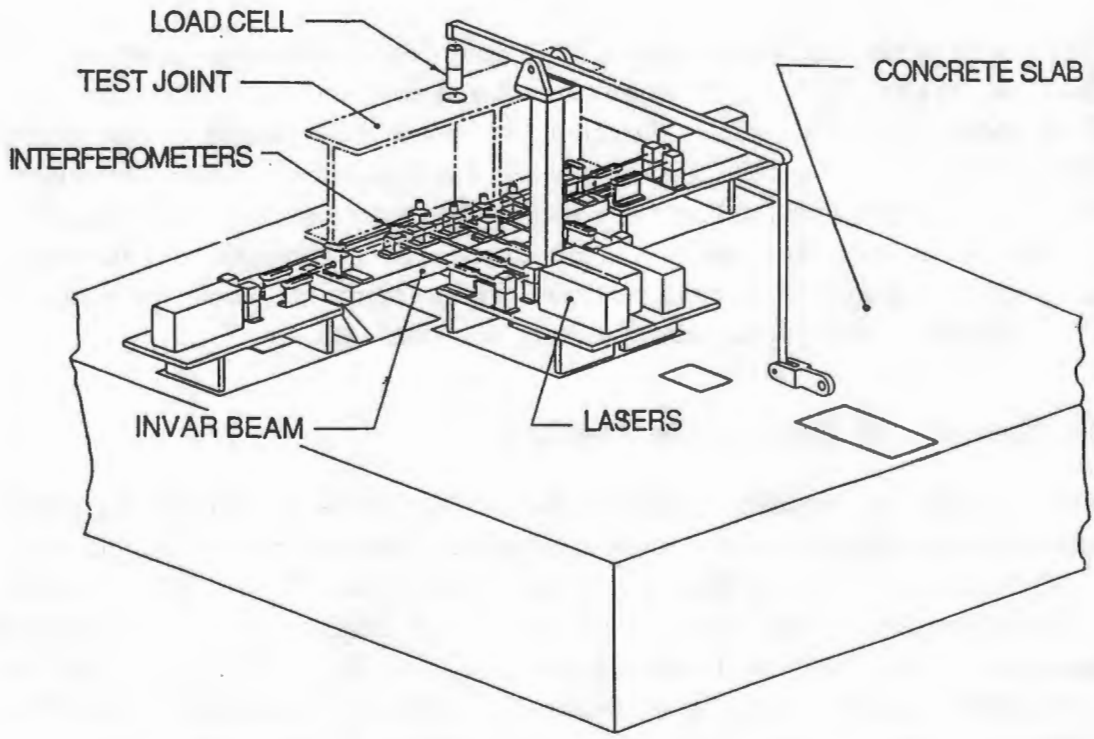

Figure 8. Hysteresis test setup

from suddenly applied and removed loadings are left for future studies.

6.1 Description of Hysteresis Test

The test was conducted at the Laser Interferometer Micro Measurement System (LIMMS) Lab. This lab is capable of measuring small displacements with a resolution of ± 0.6 micro-inches. This is achieved by using a series of Hewlett-Packard laser interferometers mounted on a seismic pad. The lasers were sampled 100 times a second and averaged over one-second intervals to eliminate high-frequency jitter influences. To help minimize temperature effects, the lab uses its own air-conditioner system, steady to ±1°F over 24 hours, and critical fixturing is made from Invar.

The test joint was supported on two blade flexures to simulate a simple support. The load was applied at the mid-span to put the joint into three-point bending. Seven lasers were used to measure displacements at varying locations along the bottom of the joint. Figure 8 is a schematic of the test setup.

Two redundant 10-pound (±0.01 lb) load cells were used; one calibrated for tension and the other for compression. Both cells were located as close to the joint interface as possible to minimize error caused by fixturing or motor drive slop or relaxation. The load was applied with a 60000-to-1 gear-reduced motor to apply a very smooth and accurate load to the joint.

The test sequence used was to zero the load fixture and take displacement readings. As load was applied laser readings were monitored continuously. When the target load was achieved in the positive direction, the motor drive paused for 10 seconds and unloaded to zero. Another 10-second pause was maintained at zero immediately followed by a negative load application to reverse the target load. The sequence would then pause at this negative load and again at zero. By cycling the load between a positive and negative load, a more realistic load environment, where the structure was not allowed to settle in any one direction, was simulated.

6.2 Results of Hysteresis Testing

The test sequence was applied at medium-to-small load levels to determine the beams response at as low of displacement levels as possible. Tests were run at ± 1,5,10,25,50, and 100 pounds. Stresses at these load levels never exceed 50 psi, which is two orders of magnitude less than the microyield strength.[4] Deflections used for hysteresis measurements were taken at the mid-span of the joint after subtraction of the end measurements, in effect zeroing any contribution of the test fixturing to deflections or hysteresis. The stiffness of the joint was measured as 142,300 lb/in, so deflections during all test runs were very small.

The data suggests that hysteresis shifts the structure in the direction of the last applied load. This observation is relatively insignificant considering the dynamic disturbance and cyclically decaying response typical of spacecraft structures.

Test runs were repeated up to 50 times each to increase confidence in the results. While every attempt has been made to minimize outside disturbances from influencing test measurements, the scatter of data levels is much greater than the laser resolution would suggest. Data scatter during higher load levels are probably caused by large disturbances such as trucks passing by the building, foot traffic down adjacent hallways, or the air conditioner switching on at an inopportune moment. Scatter in the data during the ±1-pound test is much smaller and can be caused by more sources such as load cell resolution, humidity changes and motor vibrations. To minimize the influences from all these error sources, only the data that fits within a one sigma (.68p) distribution is kept for analysis, essentially throwing out the worst one third of the data at each load level.

The remaining data is then averaged and plotted for of the six each load levels. The curve plotted for Figure 9 shows that hysteresis in the joint is typical of precision structures. The composite construction and applied damping treatment have not appreciably increased hysteresis above one percent for large disturbances. However when disturbances are less than about 0.001 inches the test data would suggest that structural hysteresis is nonlinear. The ±1 sigma error band is included to show test repeatability. Admittedly since the number of perturbating error sources and

significance of test inaccuracies increases at low disturbance levels, one would expect to see a curve shape similar to Figure 9 even if percent hysteresis is linear and constant. However the amount of nonlinearity measured is more than expected by attempting to quantify the test error sources alone.

7. Summary and Conclusions

The viscous damping in the untreated Test Joint was measured to be 0.28% for the strong-direction bending mode and 0.26% in the first twisting mode. The damping of the bending mode was shown to be constant down to a displacement level of about 5 nm zero-to-peak.

A finite element model of the Test Joint was constructed for the purpose of evaluating damping concepts for the Test Joint. Though few attempts were made to tune the model to the test results, the model predicted with good accuracy the damping in the treated Test Joint. The roughly 3-pound damping treatment resulted in about 2% viscous damping in the bending mode and about 2.5% in the lowest twisting mode.

The best quality signals for the low-level damping came from the test of the treated structure. Figure 10 shows the damping measured versus maximum zero-to-peak displacement. It is important to understand that the damping values of 1.95 and 2.04 are virtually the same within the accuracy of the test. With 1024 measurements over the frequency range of 160 to 640 Hz, the modal and half-power frequencies can only be determined to an accuracy of $\frac{(640-160)}{1024} = 0.47$ Hz. The damping is determined by $\frac{\Delta\omega}{\omega_n}$, where $\Delta\omega$ spans the half-power points and ω_n is the center (natural) frequency. Thus, the measurement of damping for the 530-Hz mode can only be resolved to within $\frac{0.47}{\omega_n} = \frac{0.47}{530} \approx 0.09\%$ viscous damping. The only deviation comes at the very lowest level, where the load levels were so small that the signal-to-noise ratio was poor; most of the response was attributed to the drive gear in the shaker.

This work demonstrates structural damping using a viscoelastic material (VEM) to be constant with respect to amplitude down to nano-meter levels. It shows that passive damping is a viable means for reducing the response of structures using this construction to external excitations. Finally, the correlation between the analysis and test shows that levels of damping can be predicted with reasonable accuracy. The collimation of the above factors gives engineers a valuable and powerful tool for analysis and design of precision structures.

Structural hysteresis of the test joint is shown in Figure 9. Plus or minus 1% hysteresis can be used as a conservative estimate to bound large-deflection hysteresis of structures using the passively damped composite construction techniques. The hysteresis behavior of these structures appears to be nonlinear at very small displacement levels. For analysis of events which produce disturbances less than one mil, Figure 9 along with an appropriate uncertainty factor can be used as a design guide.

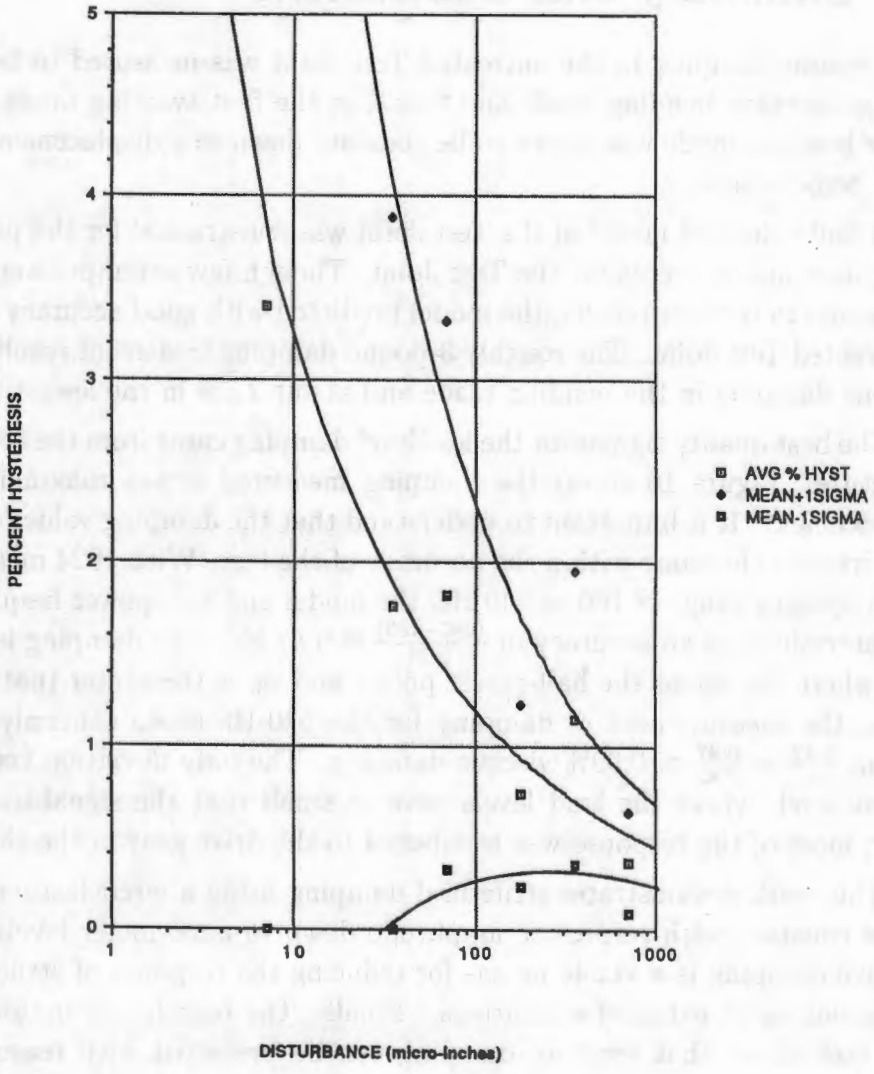

Figure 9. Hysteresis results - one sigma (0.68p)

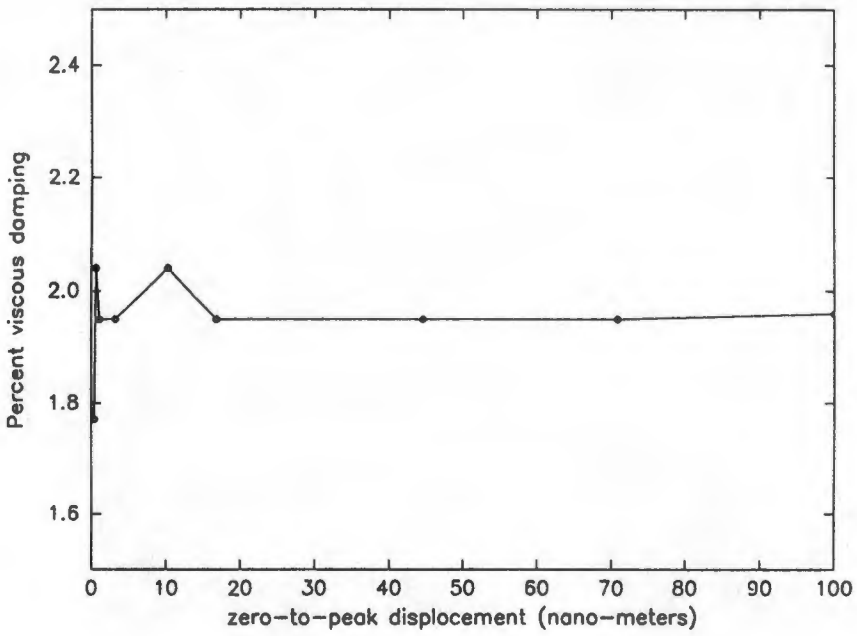

Figure 10. Damping versus maximum displacement for the treated test structure

References

[1] Lee, Stuart M., Editor, *International Encyclopedia of Composites.*

[2] Schloss, Fred, "Accelerometer Overload," *Sound and Vibration*, Page 12, January, 1989.

[3] Harris, C.M., and Crede, C.E. (eds.), *Shock and Vibration Handbook, Second Edition*, Page 22-11, McGraw-Hill, New York, 1976.

[4] Wolff, E.G. and Crane, S.T., "Prediction of the Microyield Strength of Polymer Matrix Composites," Journal of Composite Technology & Research, Vol. 10, No. 4, Winter 1988.